# Robust Navigation and Mapping Architecture for Large Environments

Favio Masson, Jose Guivant, Eduardo Nebot

F. Masson is with the Departamento de Ingeniería Eléctrica, Universidad Nacional del Sur, Argentina. E-mail: fmasson@uns.edu.ar.

J. Guivant and E. Nebot are with the Australian Centre For Field Robotics, University of Sydney, Australia. E-mail: jguivant/nebot@acfr.usyd.edu.au

July 14, 2003

**Abstract**

This paper addresses the problem of Simultaneous Localization and Mapping (SLAM) for very large environments. A Hybrid architecture is presented that makes use of the Extended Kalman Filter to perform SLAM in a very efficient form and a Monte Carlo localiser to resolve data association problems potentially present when returning to a known location after a large exploration period. Algorithms to improve the convergence of the Monte Carlo filter are presented that consider vehicle and sensor uncertainty. The proposed algorithm incorporates significant integrity to the standard SLAM algorithms by providing the ability to handle multimodal distributions over robot pose in real time while the mapping process is on hold. Experimental results in outdoor environments are presented to demonstrate the performance of the algorithm proposed.

**Keywords**

Bayes Estimation, Bootstrap Filter, SLAM, Navigation

## I. Introduction

Reliable autonomous navigation in highly unstructured outdoor environments presents formidable problems in terms of sensing, perception and navigation algorithms [1]. The problem of localization given a map of the environment or estimating the map knowing the vehicle position is known to be a solved problem and has been in fact applied in many research and industrial applications [2] [3]. Outdoor environments present additional challenges due to the lack of sensors and perception algorithms that can work reliably in all environments and under all weather conditions.

This is starting to change with sensors like Laser and Radars capable of returning 2-D and 3-D reliable and consistent information and with important progress in perception algorithms [4] [5]. Once the sensing and perception problem is addressed, the localization problem can be solved using a number of approaches. Some methods are based on the non-linear version of the Kalman Filter, the Extended Kalman Filter (EKF). Other methods use approximations of the probabilistic density of the states conditioned to the measures obtained. These approaches can be classified into three categories: the mixture of densities [6], the grid based methods [7] and the Monte Carlo methods [8].

A much more complicated problem is when both the map and the vehicle position have to be estimated. This problem is usually referred to as Simultaneous Localization and Mapping (SLAM) [9] or Concurrent Map Building and Localization (CML) [10]. This problem has also been addressed in [11] using an expectation maximization method in indoor problems and in [6] using a sum of Gaussian in sub-sea applications. These algorithms are suitable for handling multi-modal probability distribution. Although these methods have proven to be very robust in many localization applications, their extension to SLAM is computationally expensive making them difficult to apply in real time. In a recent work [12] an algorithm named FASTSlam was presented that decomposes the model into a linear part (the model of the evolution of the map) and a nonlinear part formed by the model representing the dynamic of the states of the vehicle. The results presented assume the data association is known. This gap is attempted to be filled in [13]. Another drawback is that its performance degrades when there is low correlation between landmarks and\or high uncertainty in the vehicle pose estimation. In this case a large number of particles is necessary to keep a good approximation of the real probability distribution. This situation arises when the SLAM process is applied over a large area or when the landmark population is low.

Kalman Filter approaches can be extended to solve the SLAM problem in very large environments. In [14] a Compressed Extended Kalman Filter (CEKF) algorithm was introduced that significantly reduces the computational requirement without introducing any penalties in the accuracy of the results. Sub-optimal simplifications were also presented in [15] to update the full covariance matrix of the states bounding the computational cost and memory requirements.

Although the implementation of SLAM can be made very efficient in terms of computational complexity and memory requirements, there are still fundamental problems that need to be solved. The SLAM algorithms are based on an exploration stage and re-visit of known places (closing a loop) to register the new learned map to the known

map. Depending on the quality of the kinematics models and external sensors used, the exploration stage could be extended to large areas. Nevertheless no matter how good the sensors and models are, at one point the accumulated error will make the correct data association task impossible. Although significant improvements to the standard Nearest Neighbor (NN) data association algorithm were presented in [16] there will be cases where the wrong hypothesis will be selected and the filter will have a catastrophic failure. This is an inherent limitation of all simultaneous navigation and mapping methods based on single hypothesis EKF techniques and is independent of the implementation method or model used.

Some recent papers [17][18] present algorithms addressing this problem using maximum likelihood mapping with a posterior estimation implemented with a particle filter and grid based methods respectively. Both methods present approximations of the full posterior estimation and may generate over-confident results since correlation with part of the map is not considered to make the algorithms implementable in real time. This can be taken into account in [17] by adjusting a tuning constant $K$ but at the same time it can make the algorithm very expensive in large environments.

In this paper we present a robust solution to this problem using a combination of the CEKF with a Monte Carlo Filter. This hybrid architecture is designed to exploit the efficiency of the CEKF algorithm to evaluate the full posterior vehicle and map states estimates and a Monte Carlo Filter to resolve the data association problem when required.

The Monte Carlo Filter is only activated under potential data association problems. It is initialized exploiting the known vehicle and map state statistics provided by the CEKF filter. Several techniques are presented to accelerate the convergency of the algorithm to make them very efficient for on-line applications. The algorithm is presented for generic range\bearing sensors, range only sensors and bearing only sensors.

The paper is organized as follows. Section II presents the Hybrid SLAM approach.

Section III presents the Bayes framework and the Particle Filter implementation with extensions to support range and bearing and range / bearing only sensors. Section IV presents practical considerations for real time implementation. Section V presents experimental results in outdoor unstructured environments. Finally Section VI presents conclusions.

## II. A Hybrid SLAM approach

Most EKF implementations generate state estimations with mono-modal probability distributions and are not capable of handling multimodal probability distributions. These situations are typical when closing large loops, that is, revisiting known places after a large exploration period. It is at this stage where the standard data association methods usually fail. A particle filter can address this problem since it naturally deals with multi-hypothesis problems.

The proposed hybrid architecture uses CEKF under normal conditions to perform SLAM. At a certain time the system may not be able to perform the association task due to large errors in vehicle pose estimation. This is an indication that the filter can not continue working assuming a mono-modal probability density distribution. At this time, we have the CEKF estimated mean and deviation of the states representing the vehicle pose and landmark positions. With the currently estimated map, a de-correlated map is built using a coordinate transform and the decorrelation procedures presented in [15]. A particle filter initialized using the available statistics is then used to resolve the position of the vehicle as a localization problem. When the multi-hypothesis problem is resolved the CEKF is restarted with the states values back propagated to the time when the data association problem was detected. Then the CEKF resumes operation until a new potential data association problem is detected.

Under the SLAM framework the vehicle starts at a position with known uncertainty and obtains measurements of the environment relative to its location. This information

is used to incrementally build and maintain a navigation map and to localize the vehicle with respect to this map. The system will detect new features at the beginning of the mission and when the vehicle explores new areas. Once these features become reliable and stable they are incorporated into the 2 dimensional map becoming part of the state vector. The state vector is then given by:

$$\begin{aligned} X &= \begin{bmatrix} X_L \\ \mathbf{m} \end{bmatrix} \\ X_L &= (x_L, y_L, \varphi_L)^T \in R^3 \\ \mathbf{m} &= (x_1, y_1, .., x_N, y_N)^T \in R^{2N} \end{aligned} \tag{1}$$

where $(x, y, \varphi)_L$ and $(x, y)_i$ are the states corresponding to the vehicle and $N$ features incorporated into the map $\mathbf{m}$ respectively. Since the environment is considered to be static the discrete dynamical model for the extended system has the form:

$$\begin{aligned} X_L(k+1) &= f(X_L(k), U(k)) + \gamma \\ \mathbf{m}(k+1) &= \mathbf{m}(k) \end{aligned} \tag{2}$$

Since the landmarks are assumed static the Jacobian matrix for the extended system becomes:

$$\begin{aligned} \frac{\partial f}{\partial X} &= \begin{bmatrix} \frac{\partial f}{\partial \tilde{x}_L} & \emptyset \\ \emptyset^T & I \end{bmatrix} = \begin{bmatrix} J_1 & \emptyset \\ \emptyset^T & I \end{bmatrix} \\ J_1 &\in R^{3x3}, \quad \emptyset \in R^{3xN}, \quad I \in R^{2Nx2N} \end{aligned} \tag{3}$$

These models can then be used with a standard EKF algorithm to build and maintain a navigation map of the environment and to track the position of the vehicle. It is well known that the solution of this problem using standard EKF algorithms has computational requirements of $O(N^2)$, $N$ being the states used to represent the landmarks and vehicle pose. As noted before the computational requirement can be reduced to constant time [14] almost independently of the map's size. This algorithm is very efficient when the vehicle remains in local areas for a significant period of time or when high frequency external information is incorporated.

## III. Monte Carlo Localization

The localization problem under a probabilistic estimation approach requires that the marginal probability density $p(x_{L_k}|\mathbf{m}, \mathbf{Z^k}, \mathbf{U^k}, \mathbf{x_0})$ must be known for all $k$, where $x_{L_k}$ is the vehicle state, $x_0$ its initial condition, $\mathbf{m}$ are the states representing a feature in the map and $\mathbf{Z^k}$ and $\mathbf{U^k}$ are the observations and input signals respectively at time $k$. The recursive evaluation of this density, assuming that the a priori density $p(x_{L_{k-1}}|\mathbf{m}, \mathbf{Z^{k-1}}, \mathbf{U^{k-1}}, \mathbf{x_0})$ is known is

$$\begin{aligned} &p(x_{L_k}|\mathbf{m}, \mathbf{Z^k}, \mathbf{U^k}, \mathbf{x_0}) = \kappa \mathbf{p}(\mathbf{z_k}|\mathbf{m}, \mathbf{x_{L_k}}) \\ &\int p(x_{L_k}|x_{L_{k-1}}, u_k) p(x_{L_{k-1}}|\mathbf{m}, \mathbf{Z^{k-1}}, \mathbf{U^{k-1}}, \mathbf{x_0}) \mathbf{dx_{L_{k-1}}} \end{aligned} \tag{4}$$

where $\kappa$ is a normalization constant, $p(z_k|x_{L_k}, \mathbf{m})$ represents the observation model and $p(x_{L_k}|x_{L_{k-1}}, u_k)$ models the vehicle dynamic.

Equation 4 can be implemented using Particle Filters. These filters approximate the joint posterior density using a set of random samples called particles. Theoretically, as the number of samples becomes very large, this representation tends to be exact and the filter estimation identical to the Bayesian ideal filter (eq. 4).

Several approaches have been proposed to implement this type of filter. One of such algorithms was presented by Gordon et al. [19] and is known as the *Bayesian Bootstrap Filter* or SIR (Sampling Importance Resampling). A similar algorithm, *Condensation Algorithm*, has been independently proposed by Isard and Blake [20]. In general these filters are usually known as *Monte Carlo Filters*.

The basic SIR filter algorithm [19] can be described as follows. A set of samples or "particles" is obtained from the prior density distribution. These particles are propagated through the system equations and assigned a weight proportional to their likelihood. Then a resampling stage is used to reduce the set of weighted particles to a set of equally weighted particles. This set can be thought of as an approximate sample for the posterior distribution and is used as the starting point for the next iteration of the algorithm. One

of the main advantages of the particle filter is the ease with which it can be applied to most estimation problems. The algorithm is straightforward and the class of models it can be applied to is very large. It is also possible to use algorithms with computation complexity of $O(R)$ where $R$ is the number of particles [21].

In this work we use the SIR filter approach presenting methods to improve the initial distribution of particles and to reduce the computer complexity for the filter implementation in real time and its interface with the CEKF for SLAM applications.

### *A. Localization with the Particle Filter*

Particle Filters approximate the joint posterior density with a set of random samples called particles. As the number of samples becomes large, they provide a practically exact and equivalent representation of the required distribution, that is the filter output will be close to the Bayesian filter. In this work we use the SIR (Sampling Importance Resampling) filter [19] to localize a vehicle in a predefined map using range and/or bearing information. Assuming that $R$ samples $\{x_{k-1}^i\}_{i=1}^R$ of the previous posterior distribution are available, the process model is then used to propagate these samples to obtain $\{\tilde{x}_k^i\}_{i=1}^R$. The new samples represent the *a priori* probability density $p(x_k|\mathbf{m}, \mathbf{Z^{k-1}}, \mathbf{U^k}, \mathbf{x_0})$.

The update stage is performed in two steps. The first step consists of the evaluation of the likelihood for each predicted particle as,

$$w_i = \frac{p(z_k|\mathbf{m}, \tilde{\mathbf{x}}_\mathbf{k}^\mathbf{i})}{\sum_{j=1}^{R} p(z_k|\mathbf{m}, \tilde{\mathbf{x}}_\mathbf{k}^\mathbf{j})} \tag{5}$$

where $z_k$ is the observation at time $k$. The pair $\{\tilde{x}_k^i\}_{i=1}^R$ , $\{w_k^i\}_{i=1}^R$ defines a discrete distribution that tends to the real continuous *posterior* distribution as $R$ tends to infinity.

The second stage performs a resampling by selecting only the particles with probability $p_r\{x_k^j = \tilde{x}_k^i\} = w_k^i$ for each $j$. Algorithms that perform this stage with computational complexity $\propto R^2$ and $\propto R$ can be found in [19] and [21] respectively.

Finally the probability of measuring $z_k$ given the state $\tilde{x}_k$ is required, that is $p(z_k|\mathbf{m}, \tilde{\mathbf{x}}_\mathbf{k}^\mathbf{i})$.

This pdf can be approximated with a sum of Gaussian (SOG) assuming each beacon is represented with a Gaussian distribution centered at its estimated position and considering all the uncertainties present in the observation:

$$p(z_k|\mathbf{m}, \mathbf{x_{L_k}}) = \sum_{\mathbf{1}}^{\mathbf{n}} \frac{\alpha_\mathbf{i}}{\mathbf{2}\pi\sigma_\mathbf{r}\sigma_\beta} \mathbf{e}^{-\mathbf{0.5}(\frac{(\mathbf{x_m}-\mathbf{x_i})^\mathbf{2}}{\sigma_\mathbf{x}^\mathbf{2}}+\frac{(\mathbf{y_m}-\mathbf{y_i})^\mathbf{2}}{\sigma_\mathbf{y}^\mathbf{2}})} \tag{6}$$

where $(x_i, y_i)$ are the landmarks a priori estimated positions, $\sigma_x$ and $\sigma_y$ are the correspondent deviation in $x$ and $y$ and $(x_m, y_m)$ are the observations obtained from each particle. For the range and bearing case they can be expressed as follows:

$$\begin{aligned} x_m &= \tilde{x_{L_k}}^i + z_r \cos(z_\beta - pi/2 + \tilde{\varphi_{L_k}}^i) \\ y_m &= \tilde{y_{L_k}}^i + z_r \sin(z_\beta - pi/2 + \tilde{\varphi_{L_k}}^i) \end{aligned} \tag{7}$$

where $(\tilde{x_{L_k}}^i, \tilde{y_{L_k}}^i, \tilde{\varphi_{L_k}}^i)$ are each of the states of the particles and $(z_r, z_\beta)$ are the observations. The sum of Gaussians 6 is augmented with a *virtual beacon* centered at the origin of the map and represented by a Gaussian with very large deviation. This is to overcome the problem of observing an object with no correspondence in the map. The following sub-sections present the localization equations that consider uncertainty in the position of the landmarks in addition to the noise in the observations.

### A.1 Localization with Range and Bearing Information

For the case of range and bearing observation $(z_r, z_\beta)$, we considered that the measurements are contaminated by additive noise $(\gamma_r, \gamma_\beta)$ with a given probability distribution. The conditional probability distribution of the observation $(z_r, z_\beta)$ with respect to the vehicle states, considering the uncertainty in the landmark position and the observation noise, can be obtained from the following integral,

$$\begin{aligned} p(z_k|\mathbf{m}, \mathbf{x_{L_k}}) &= \int_{\mathbf{\Omega}} \mathbf{p}(\mathbf{m_x}, \mathbf{m_y}, \gamma_\mathbf{r}, \gamma_\beta)\ \mu\ |\overrightarrow{dS}| \\ \Omega &= \{(\mathbf{m_x}, \mathbf{m_y}, \gamma_\mathbf{r}, \gamma_\beta) \in \Re^\mathbf{4}\} \end{aligned} \tag{8}$$

Equation 8 is a surface integral and $p(\mathbf{m_x}, \mathbf{m_y}, \gamma_\mathbf{r}, \gamma_\beta)$ is the joint probability density distribution of the random variables (r.v.) due to the four noise sources. The factor

$\mu \cdot |\overrightarrow{dS}|$ is the surface differential used to perform the integration over the surface region defined by the equality constraint given in equation 9.

$$\begin{aligned} z_r &= \sqrt{(\mathbf{m_x} - \mathbf{x_L})^2 + (\mathbf{m_y} - \mathbf{y_L})^2} + \gamma_r \\ z_\beta &= \arctan(\tfrac{\mathbf{m_y} - \mathbf{y_L}}{\mathbf{m_x} - \mathbf{x_L}}) - \varphi + \tfrac{\pi}{2} + \gamma_\beta \end{aligned} \tag{9}$$

The probability density distribution given in Equation 8 can be evaluated using the probability density distribution restricted to the observations,

$$p_{z_r,z_\beta}(z_{r_0}, z_{\beta_0}) = \frac{\partial F_{z_r,z_\beta}(z_{r_0}, z_{\beta_0})}{\partial z_r \partial z_\beta} \tag{10}$$

where $F_{z_r,z_\beta}(z_{r_0}, z_{\beta_0})$ is the probability distribution. After some manipulations this distribution can be expressed as

$$\begin{aligned} &F_{z_r,z_\beta}(z_{r_0}, z_{\beta_0}) = \\ &\int_{-\infty}^{\infty}\int_{-\infty}^{\infty}\int_{-\infty}^{\gamma r_0}\int_{-\infty}^{\gamma r_0} p(\mathbf{m}_x, \mathbf{m}_y, \gamma_r, \gamma_\beta) \cdot d\gamma_r \cdot d\gamma_\beta \cdot d\mathbf{m}_x \cdot d\mathbf{m}_y \\ &\gamma_{r_0} = z_{r_0} - \sqrt{(m_x - x_L)^2 + (m_y - y_L)^2}, \\ &\gamma_{\beta_0} = z_{\beta_0} - \arctan(\tfrac{m_y - y_L}{m_x - x_L}) + \varphi - \tfrac{\pi}{2}, \end{aligned} \tag{11}$$

The integral argument is the probability density distribution of the four r.v.,

$$p(\mathbf{m}_x, \mathbf{m}_y, \gamma_r, \gamma_\beta) = p_{\mathbf{m}_x,\mathbf{m}_y,\gamma_r,\gamma_\beta}(\mathbf{m}_x, \mathbf{m}_y, \gamma_r, \gamma_\beta) \tag{12}$$

Finally, the probability density distribution is evaluated by differentiating the probability distribution function (11),

$$\begin{aligned} &p_{z_r,z_\beta}(z_{r_0}, z_{\beta_0}) = \tfrac{\partial F_{z_r,z_\beta}(z_{r_0}, z_{\beta_0})}{\partial z_r \partial z_\beta} = \\ &\int_{-\infty}^{\infty}\int_{-\infty}^{\infty} p(\mathbf{m}_x, \mathbf{m}_y, \gamma_{r_0}(\mathbf{m}_x, \mathbf{m}_y), \gamma_{\beta_0}(\mathbf{m}_x, \mathbf{m}_y)) d\mathbf{m}_x d\mathbf{m}_y \end{aligned} \tag{13}$$

The integral evaluation 13 can be simplified by reducing the integration region to the $\mathbf{m}_x, \mathbf{m}_y$ space close to the landmarks. This simplification is valid provided that the pdf $p_{\mathbf{m}_x,\mathbf{m}_y}(\mathbf{m}_x, \mathbf{m}_y)$ is approximated by a sum of Gaussians pdf's (SOG). In this work a

region of size $2\sigma$ deviation centered at the expected position of the landmark is used. The probability density distribution $p_{\mathbf{m}_x,\mathbf{m}_y}(\mathbf{m}_x, \mathbf{m}_y)$ becomes negligible outside these regions.

### A.2 Localization with bearing only information

In this case the estimation of the vehicle position and velocity is based on a series of bearing only observations. Examples of this type of sensor are video cameras and certain types of lasers. The lack of range information makes localization a very difficult problem. The observations model in 2-D is

$$z_{\beta_j} = \varphi_L - \arctan\frac{y_i - y_L}{x_i - x_L} + \frac{\pi}{2} \tag{14}$$

where $(x_i, y_i)$ represents the position of the beacon $i$, $(x_L, y_L, \varphi_L)$ is the vehicle pose and $\beta_j$ is the observed bearing to the beacon $j$. The probability $p(z_k|x_{L_k})$ can be calculated similarly to (eq. 13) considering all the sources of uncertainties

$$p_{z_\beta}(z_{\beta_0}) = \int_{-\infty}^{\infty}\int_{-\infty}^{\infty} p(\mathbf{m}_x, \mathbf{m}_y, \gamma_{\beta_0}(\mathbf{m}_x, \mathbf{m}_y)) \cdot d\mathbf{m}_x \cdot d\mathbf{m}_y \tag{15}$$

where

$$\gamma_{\beta_0} = \gamma_{\beta_0}(\mathbf{m}_x, \mathbf{m}_y) = \beta - \arctan\left(\frac{\mathbf{m}_y - y_L}{\mathbf{m}_x - x_L}\right) + \varphi_L - \frac{\pi}{2} \tag{16}$$

### A.3 Localization with range only information

Other common types of sensors are those that return range only information or range and bearing but with large uncertainty in bearing such as ultrasonic sensors. The observations model can then be written

$$z_{r_j} = \sqrt{(y_i - y_L)^2 + (x_i - x_L)^2} \tag{17}$$

where $(x_i, y_i)$ is the position of the observed beacon $i$, $(x_L, y_L, \varphi_L)$ is the vehicle position and $z_{r_j}$ is the $j$ observation in the sensor data frame.

The conditional probability density distribution $p(z_k|x_{L_k})$ can be calculated according to (eq. 18) considering all the uncertainties present

$$p_{z_r}(z_{r_0}) = \int_{-\infty}^{\infty}\int_{-\infty}^{\infty} p(\mathbf{m}_x, \mathbf{m}_y, \gamma_{r_0}(\mathbf{m}_x, \mathbf{m}_y)) \cdot d\mathbf{m}_x \cdot d\mathbf{m}_y \tag{18}$$

where

$$\gamma_{r_0} = z_{r_0} - \sqrt{(\mathbf{m}_x - x_L)^2 + (\mathbf{m}_y - y_L)^2} \tag{19}$$

## IV. Practical implementation

This section presents several important implementation issues that need to be taken into account to maximize the performance of the hybrid architecture presented. These are the transformation of the relative to absolute map and the determination of the area of interest, the particle initialization and interface between the CEKF and the particle filter. The solutions presented consider the uncertainties in vehicle, map and sensor to maximize the number of particles in the most likely position of the vehicle.

### *A. Map for the particle filter*

The SLAM algorithm builds a map while the vehicle explores a new area. The map states will be, in most cases, highly correlated in a local area. In order to use the particle filter to solve the localization problem, a two dimensional map probability density distribution needs to be synthesized from an originally strongly correlated $n$ dimension map. The decorrelation procedure is implemented in two steps. The map, originally represented in global coordinates is now represented in a local frame defined by the states of two beacons that are highly correlated to all the local landmarks. The other local landmarks are then referenced to this new base. This results in a covariance matrix of the form,

$$p\mathbf{m} = \begin{bmatrix} \mathrm{p}_{\mathbf{m}_1} & C_{12} & \cdots & C_{1m} \\ C_{21} & \mathrm{p}_{\mathbf{m}_2} & \cdots & \vdots \\ \vdots & \ddots & \ddots & \vdots \\ C_{m1} & \cdots & \ddots & \mathrm{p}_{\mathbf{m}_\mathrm{m}} \end{bmatrix} \tag{20}$$

where the cross-correlation components between states of different landmarks are usually weak, i.e. they meet the condition $C_{i,j}/\sqrt{p_{m_i} \cdot p_{m_j}} << 1$. To de-correlate the map it is necessary to apply an additional step. A conservative bound matrix for (eq. 20) can be easily obtained increasing the diagonal components and deleting the cross-correlation terms. This can be implemented as shown in eq 21 where $diag[\cdot]$ represents the elements of a diagonal matrix [15]. For presentation purposes, all the states in equation 21 are assumed to belong to different landmarks. The decorrelation procedure performs the decorrelation of block diagonal matrices, each block matrix being the covariance of the states representing a particular landmark. Then, each state is decorrelated with respect to all the other states except from the states that correspond to its associated landmark.

$$\tilde{p}\mathbf{m} = diag \begin{bmatrix} p\mathbf{m}_1 + \sum_{j}^{j \neq 1} \mid k_{1j} \cdot C_{1j} \mid \\ \vdots \\ p\mathbf{m}_m + \sum_{j}^{j \neq m} \mid k_{mj} \cdot C_{mj} \mid \end{bmatrix} \tag{21}$$

The set $\{k_{ij}\}_{i,j}$ meets the condition $k_{ij} = 1/k_{ji} > 0$. This *un-correlated* map is used to define a two dimension map probability density distribution used by the particle filter to localize the vehicle.

### *B. Particle Filter Initialization*

As the number of particles affects both the computational requirements and convergence of the algorithm, it is necessary to select an appropriate set of particles to represent the a priori density function at time $T_0$, that is, the time when the data association fails. Since the particle filters work with samples of a distribution rather than its analytic

expression it is possible to select the samples based on the most probable initial pose of the rover. A good initial distribution is a set of particles that is dense in at least a small sub-region that contains the true states value. The initial distribution should be based in the position and standard deviations reported by the CEKF, and in at least one observation in a sub-region that contains this true states value. In [22] a localization approach is presented that replaces particles with low probability with others based in the observations. Although this algorithm is very efficient it considers that the identity of that landmark is given ( known data association). This is true in some applications such as the one addressed in this paper but not common in natural outdoor environments where landmarks have similar aspects and the presence of spurious objects or new landmarks is common. In this paper the data association is implicitly done by the localization algorithm. The multi-hypotheses considered are defined by the uncertainty of the robot pose estimation. In addition the method presented is able to deal with false observations. Spurious observations and landmarks that do not belong to the map are naturally rejected by the localizer. The technique presented in our paper considers the information from a set of observations to select all particles, *not to replace some*, only in the initial distribution and combined with the CEKF estimates as was mentioned previously. In fact, our localization filter is a Monte Carlo Localization.

The initial distribution is created from range / bearing observations of a set of landmarks. This probability distribution is dominant in a region that presents a shape similar to a set of helical cylinders in the space $(x, y, \varphi)$. Each helix centre corresponds to a hypothetical landmark position with its radio defined by the range observation (Figure 1). The landmarks considered are only the ones that the vehicle can "see" from the location reported by the CEKF and within the range and field of view of the sensors.

Although it is recognized that some observations will not be due to landmarks, all range and bearing observations in a single scan are used to build the initial distribution. Even though a set of families of helices will introduce more particles than a single family of

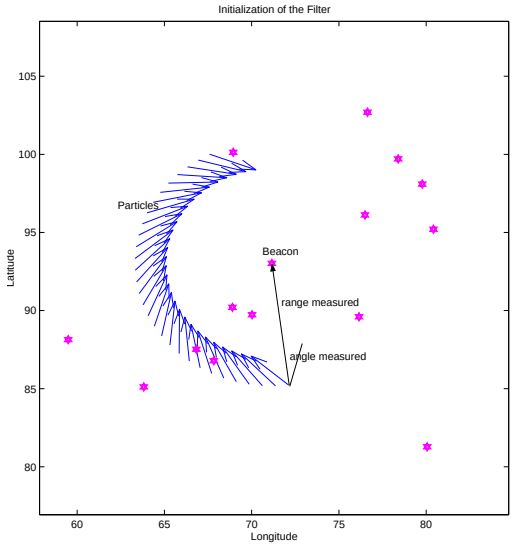


Fig. 1. Helix conformation with one measure and one beacon

helices (one observation), it will be more robust in the presence of spurious observations. By considering that the range / bearing observations are perfect then the dominant region becomes a discontinuous one dimensional curve (family of helices) $C$, in the three dimensional space $(x, y, \varphi)$

$$C = \bigcup_{i=1}^{N} C_i$$

$$C_i = \left\{ (x, y, \varphi) \setminus \begin{array}{l} x = x(\tau) = x_i + z_r \cdot \cos(\tau) \\ y = y(\tau) = y_i + z_r \cdot \sin(\tau) \\ \varphi = \varphi(\tau) = \tau - z_\beta - \frac{\pi}{2} \\ \tau \in [0, 2\pi) \end{array} \right\} \tag{22}$$

These regions can be reduced by adjusting the variation of $\tau$ according to the uncertainty in $\varphi$. Assuming the presence of noise in the observations and in the landmark positions

$$\begin{array}{c} z_r = z_r^* + \gamma_r, \quad z_\beta = z_\beta^* + \gamma_\beta \\ x_i = x_i^* + \gamma_{x_i}, \quad y_i = y_i^* + \gamma_{y_i} \end{array} \tag{23}$$

this family of helices becomes a family of cylindrical regions surrounding the helices as shown in Figure 2. The helical cylinder section can be adjusted by evaluating its

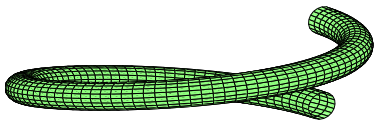

Fig. 2. Helix initialization considering the noise in the observations

sensitivity to the noise sources $\gamma_{x_i}, \gamma_{y_i}, \gamma_r, \gamma_\beta$.

The same assumptions can be made for the case of using bearing only observations. $\varphi_L$ can be expressed as a function of the observations, beacons and vehicle position. Assuming perfect observations, equation 24 defines a surface in the state space.

$$S = \{(x_L, y_L, \varphi_L) | \varphi_L = \arctan \frac{y_i - y_L}{x_i - x_L} - z_{\beta_j} + \frac{\pi}{2}\} \tag{24}$$

Although this method can be more efficient than the standard uniform o Gaussian distribution it is still very demanding in the number of particles. A more efficient algorithm can be designed considering two observations at a time. This leads to the following equations,

$$\begin{aligned} \varphi_L &= \arctan \tfrac{y_i - y_L}{x_i - x_L} - z_{\beta_a} + \tfrac{\pi}{2} \\ \varphi_L &= \arctan \tfrac{y_k - y_L}{x_k - x_L} - z_{\beta_b} + \tfrac{\pi}{2} \end{aligned} \tag{25}$$

Since the observations belong to a single scan it can be assumed that they are obtained from the same location. The intersection of the two surfaces defines a curve in the three-dimensional space of the states (eq. 26).

$$C = \{(x, y, \varphi) | x = x(\varphi), y = y(\varphi), \varphi \in [0, 2\pi)\} \tag{26}$$

This is the ideal case of no observation noise and landmarks location perfectly known,

that is:

$$\begin{cases} \varphi \in [0, 2\pi) \\ \gamma_{\beta_a} = 0 \\ \gamma_{\beta_b} = 0 \\ (x_i, y_i) = \left(x_i^0, y_i^0\right) \\ (x_k, y_k) = \left(x_k^0, y_k^0\right) \end{cases} \tag{27}$$

By considering the noise in the bearing observations and in the landmark positions, $x$ and $y$ can be expressed as in (eq. 28)

$$\begin{aligned} \rho_1 &= \varphi + z_{\beta_a} - \pi/2 + \gamma_{\beta_a} \\ \rho_2 &= \varphi + z_{\beta_b} - \pi/2 + \gamma_{\beta_b} \\ x\left(\varphi, \gamma_{\beta_a}, \gamma_{\beta_b}, x_i, y_i, x_k, y_k\right) &= \frac{-x_k \cdot \sin(\rho_2) \cdot \cos(\rho_1) + x_i \cdot \sin(\rho_1) \cdot \cos(\rho_2) + (y_k - y_i) \cdot \cos(\rho_1) \cdot \cos(\rho_2)}{\sin(\rho_1) \cdot \cos(\rho_2) - \sin(\rho_2) \cdot \cos(\rho_1)} \\ y\left(\varphi, \gamma_{\beta_a}, \gamma_{\beta_b}, x_i, y_i, x_k, y_k\right) &= y_i - (x_i - x) \cdot \sin(\rho_1)/\cos(\rho_1) \end{aligned} \tag{28}$$

where $\varphi \in [0, 2\pi)$, $\gamma_{\beta_a}$ and $\gamma_{\beta_b}$ are r.v. with probability density $f_\beta(\gamma_\beta)$, $(x_i, y_i)$ are r. v. with probability density $f_{\mathbf{m}}(x_i, y_i)$ and $(x_k, y_k)$ are r.v. with probability density $f_{\mathbf{m}}(x_k, y_k)$.

Taking into account the different sources of noise, the curve transforms into a region that is named curved cylinder. With no data association a pair of observations will generate a family of curved cylinders to cover all possible hypotheses. It is possible to generate a sample of this distribution by applying equation 28 to samples of the six r. v.

The multi-hypothesis nature of the distribution $f_L(\cdot)$ will generate a family of regions (each region surrounding an ideal noiseless curve). This initialization is significantly less expensive than a uniform distributed sample in a large rectangular region in the $(x, y, \varphi)$ space or even a Gaussian distribution in this region. An example of this type of initialization is shown in Figure 10 in section V.

In the case of range only observations, the initialization is very similar to the range and bearing problem. In this case the main difference is in the evaluation of the orientation.

Equation (22) is modified as in Eq. (29) to take into account the range only observation.

$$C_i = \left\{ \begin{array}{c} (x, y, \varphi) \quad \backslash \\ \\ x = x(\tau) = x_i + z_r \cdot \cos(\tau) \\ y = y(\tau) = y_i + z_r \cdot \sin(\tau) \\ \varphi = \varphi(\tau) = \tau \\ \tau \in [0, 2\pi) \end{array} \right\} \tag{29}$$

*C. Selection of a reduced local map*

In most practical cases the local map is very large when compared to the sensor field of view. Most of the landmarks are usually beyond the range of the sensor. It is then possible to select only the *visible beacons* from the entire map by considering the estimated uncertainties. This will significantly reduce the computation complexity for the evaluation of equation (13). The boundaries of the reduced map are fixed based on the beacons that are close to the vehicle location, the particles position, the observation and their respective uncertainty. Figure 3 shows this approach for the case of only two particles. In this Figure $(R_i, \beta_i)$ are the observations, the " $*$ " are the projected observation from each particle and the encircled stars are the beacons. It can be noted from the Figure that only a few beacons are within the field of view of any of the particles. The other beacons are not considered to be part of the reduced map.

*D. Interface with the CEKF*

Two main issues need to be addressed to implement the switching strategy between the CEKF and the SIR filter. The first problem involves the detection of a potential data association failure while running the CEKF. This is implemented in this work by monitoring the estimated error in vehicle and local map states and the results of the standard data association process. The second issue is the reliable determination that

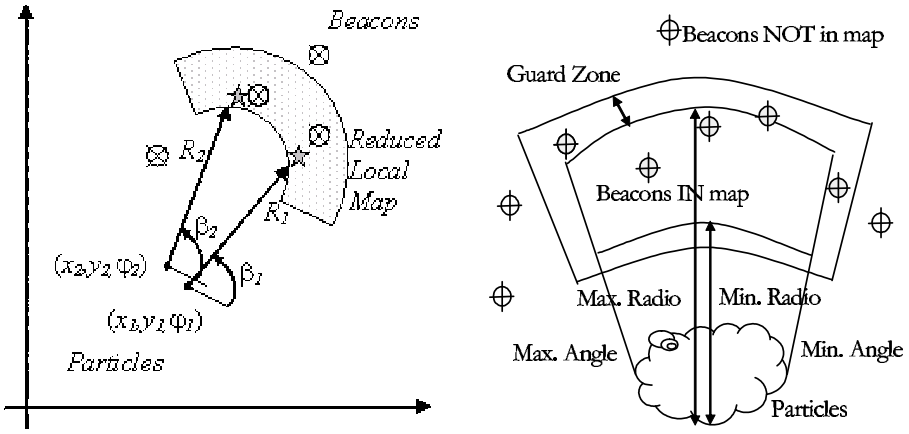


Fig. 3. Selected beacons in a reduced local map

the particle filter has resolved the multi-hypothesis problem and is ready to send the correct position to the CEKF back propagating its results. This problem is addressed by analyzing the evolution of the estimated standard deviations. The filter is assumed to converge when the estimated standard deviation error becomes less than two times the noise in the propagation error model for $x$, $y$ and $\varphi$. The convergence of the filter is guaranteed by the fact that the weights (eq. 5) are bounded above at any instant of time [23]. These weights are obtained from the integral given in equation (13). This integral is always different from zero since it is calculated over a distribution that is zero only at $\pm\infty$ making the weights to be bounded by 1.

## V. Experimental Results

This section presents experimental results obtained using the hybrid architecture in the outdoor environment shown in Figure 4. The environment is populated by trees that are used as the most relevant features to build a navigation map [24]. Full details of the vehicle and sensor model used for this experiment are available in [25].

The CEKF filter is used to navigate when no potential data association faults are detected. When a data association failure is detected the particle filter is initialized according to the procedure presented in section IV-B and is run until convergence is

Fig. 4. Experimental run in an outdoor environment

reached. At this point the filter reports the corrections to the CEKF that continue the SLAM process using EKF based methods.

The algorithms were tested in an environment with areas of different feature density as shown in Figure 5. In this experiment we logged GPS, laser and dead reckoning information. The GPS used is capable of providing position information with 2 cm accuracy. This information is only available in relatively open areas and is shown in Figure 5 with a thick line. The vehicle started at the point labeled "Starting Position" and the filter used GPS, laser and dead reckoning to perform SLAM [24] until it reached the location at coordinates -30,60 where GPS is no longer available. The SLAM remained operating using Laser and dead-reckoning information only. High accuracy GPS was again available close to the end of the run and will be essential to demonstrate the consistency and performance of the hybrid navigation architecture proposed.

The stars and encircled stars in Figure 5 represent the natural features incorporated into the map and the selected landmarks whose deviations are shown in Figure 6 respectively. A diamond and a square represent the starting and ending position resulting from the particle filter correction and are clearly shown in Figure 7. The beacons that produce the association failure are the squared stars marked as C in the figure.

Figure 8 presents the vehicle position estimated error. It can be seen that the error

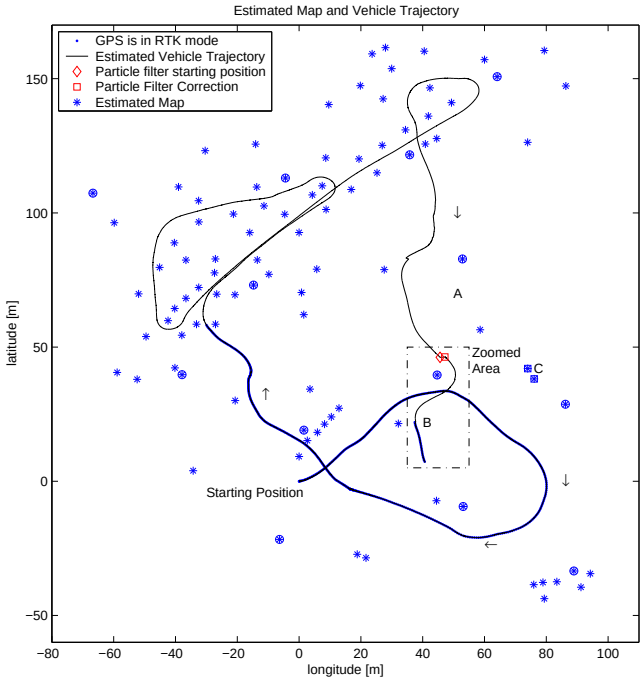


Fig. 5. Experimental run implementing SLAM using all the available information.

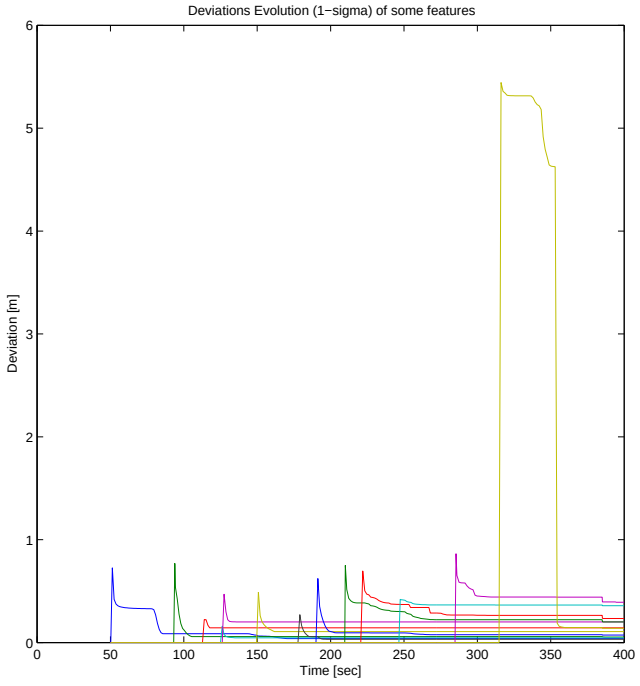


Fig. 6. Standard deviation of selected beacons in the map. These beacons are shown as rounded stars in figure 5

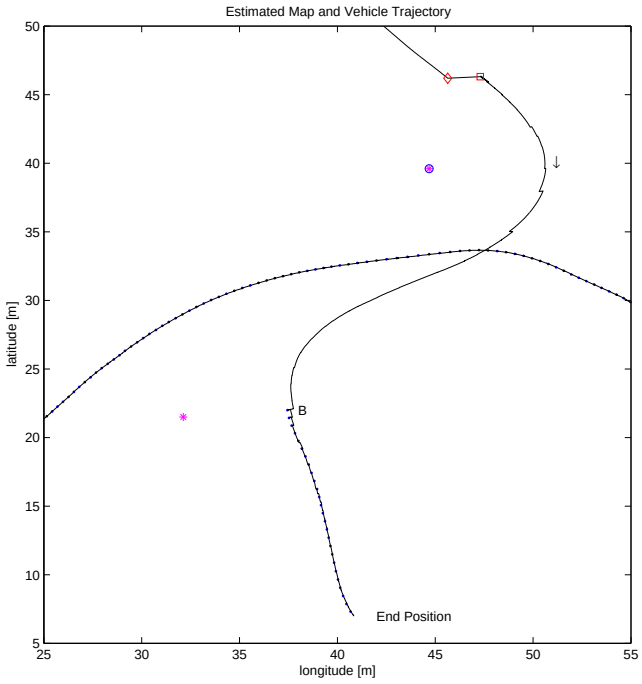


Fig. 7. A zoomed area of figure 5. A diamond and a square show the start and end position respectively of the particle filter correction. The dots represents the RTK GPS information.

was very small when the system was operating with GPS, $time < 200sec$. It is then maintained below 0.5 m while in the area with high feature density. The error then started to increase before reaching point "A" since the laser cannot detect any known feature. At this time ( 320 sec) a new feature was incorporated but with large uncertainty as shown in Figure 6. Then a known landmark was detected and since it can be associated correctly, the error in vehicle and landmark position dramatically decreased as expected. A different situation is presented in Figure 7 that corresponds to the area marked as zoomed area in Figure 5. Once the laser stoped seeing the previous known landmarks the error built up again to the point where the system can no longer associate the detected landmarks to a single known landmark. The location of the vehicle at this time is represented as a diamond at coordinates (45,45) in this figure. In this case the system has to activate the Monte Carlo localiser to generate the relocalization results shown as a square at coordinates (47,45) in the same figure.

Examples of the Monte Carlo filter initialisation are shown in Figures 9 and 10. Figure 9 shows the initialization for the range and bearing case. The figure clearly shows the helical shape of the initial distributions. The arrows represent the position and orientation of the vehicle and the stars the beacons present in the map. The initialization for the case of bearing only is also shown in Figure 10.

The relocalisation result is then reported to the CEKF to continue with the SLAM process for the rest of the run. At the end of the trajectory high accuracy GPS was again available (thick line). It can be clearly seen, specially in Figure 7, that the estimated vehicle pose just before GPS became available is very close to the high accuracy GPS reported position. This demonstrates the performance and consistency of the hybrid architecture proposed.

It is also interesting to test the algorithm in the case where the available information is not enough to select the correct hypothesis in a single scan. This is the case of using bearing only sensors. Figure 11 presents the average position of the vehicle across a Monte Carlo simulation consisting of 50 runs as a full line. The dotted line is the differential GPS position taken as a reference to verify the operation of the filter. Although the vehicle started at 0,0 the mean is not representative of the most probable position of the car during the initial part of the trajectory due to the multi-modal nature of the distribution during this period. Figure 12 shows the standard deviations of the states $x$ and $y$ of the vehicle averaged over the fifty runs. It is important to note that although the environment can be crowded with landmarks and other spurious objects the algorithm remains robust since no data association is performed at this stage. The convergence for the bearing only case is slower than the range and bearing case but it is still achieved in a few scans. The convergence time will depend on the number of features in the environment.

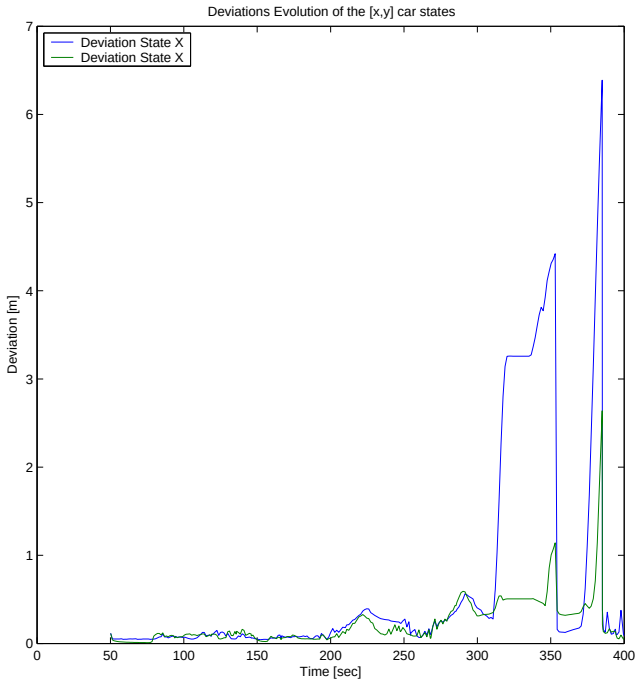


Fig. 8. Deviation of the car positions over time

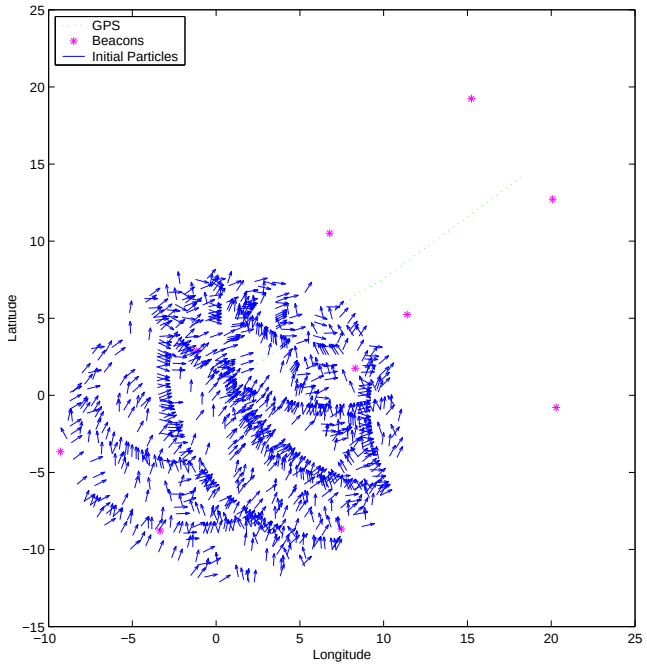


Fig. 9. Initialization of the particle filter using range and bearing information

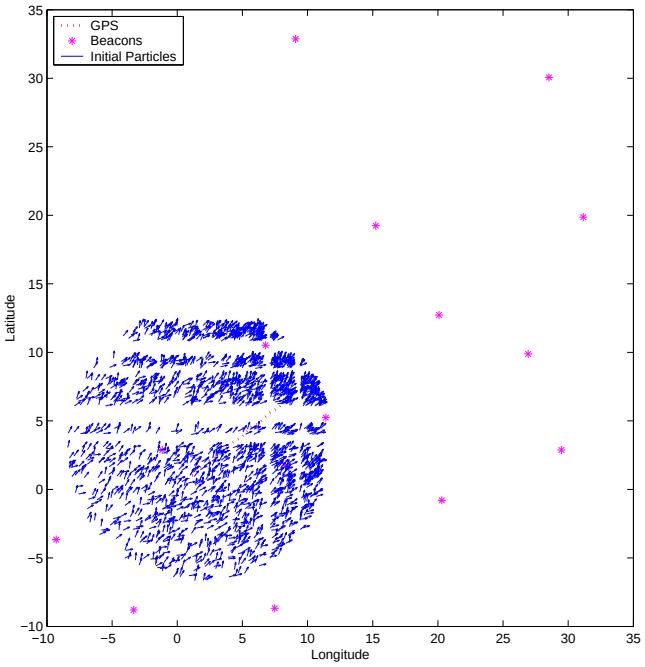


Fig. 10. Initialization of the particle filter using bearing only information

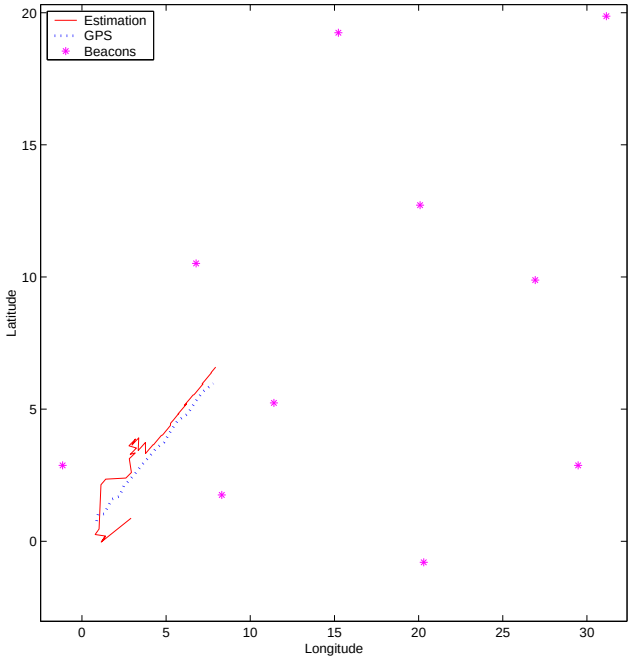


Fig. 11. The mean robot pose (averaged over 50 runs) for the bearing only localizator

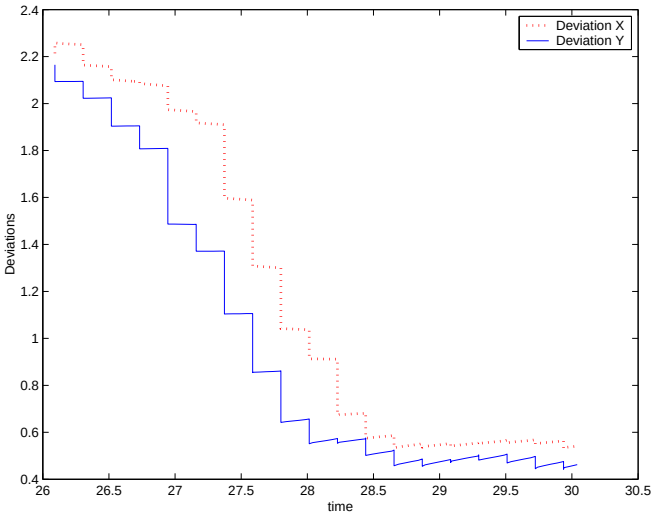


Fig. 12. History of state's $x$ and $y$ error when the filter is run with bearing only information

## VI. Conclusions

This paper presented a hybrid architecture that makes use of the Compressed Extended Kalman Filter (CEKF) algorithm to perform SLAM in an efficient form and a Monte Carlo type filter to resolve the data association problem that is normally present when the vehicle closes a large loop. The experimental results have shown that this approach can be used to increase the integrity of EKF based systems by providing the capability to temporarily handle multi-mode probability distributions.

Three factors affect the computational requirements and convergence of the algorithm. The initialization, the number of particles and the number of beacons that can be measured in a laser scan.

It was shown that a good initialization is essential to assure the convergence of the algorithm with a given number of particles. In the runs performed using range and bearing information the filter resolved the multi-hypothesis in only one laser scan. This result can be extrapolated to the case of bearing only information and range only information. The results with bearing only and range only sensors are relevant since there is a wide variety of inexpensive sensors that can be used to aid navigation systems to recover when

closing large loops. Research in under way to address the other two issues.

## References


[1] R. Chatila, "Autonomous navigation in natural environments," *Robotics and Autonomous Systems*, vol. 16, pp. 197–211, 1995.

[2] A. Elfes, *Occupancy Grids: A probabilistic framework for robot perception and navigation*, Ph. d. thesis, Department of Electrical Engineering, Carnegie Mellon University, 1989.

[3] H. F. Durrant-Whyte, "An autonomous guided vehicle for cargo handling applications," *Int. Journal of Robotics Research*, vol. 15, no. 5, pp. 407–441, 1996.

[4] J. Leonard, P. Neuman, R. Rikoski, J. Neira, and J. Tardós, "Towards robust data association and feature modeling for concurrent mapping and localization," *Proc. Tenth International Symposium of Robotics Research (ISRR'01)*, November 2001, Lorne, Australia.

[5] C. Wang and C. Thorpe, "Simultaneous localization and mapping with detection and tracking of moving objects," *IEEE International Conference on Robotics and Automation*, May 2002.

[6] Hugh Durrant-White, S. Majumder, S. Thrun, M. De Battista, and S. Scheding, "A bayesian algorithm for simultaneous localization and map building," *Proc. Tenth International Symposium of Robotics Research (ISRR'01)*, November 2001, Lorne, Australia.

[7] W. Burgard, D. Fox, D. Hennig, and T. Schmidt, "Estimating the absolute position of a mobile robot using position probability grids," *Proc. of the Fourteenth National Conference on Artificial Intelligence*, vol. 2, pp. 896–901, 1996.

[8] F. Dellaert, D. Fox, W. Burgard, and S. Thrun, "Monte carlo localization for mobile robots," *Proceedings of the 1999 IEEE International Conference on Robotics & Automation*, pp. 1322–1328, 1999.

[9] Jose Guivant, E. Nebot, and H. Durrant-Whyte, "Simultaneous localization and map building using natural features in outdoor environments," *Proc. IAS-6 Intelligent Autonomous Systems*, pp. 581–586, 25-28 Jul 2000.

[10] J. J. Leonard and H. J. S. Feder, "A computationally efficient method for large-scale concurrent mapping and localization," *Ninth International Symposium on Robotics Research*, pp. 316–321, October 1999.

[11] S. Thrun, D. Fox, and W. Bugard, "Probabilistic mapping of and environment by a mobile robot," *Proc. Of 1998 IEEE, Belgium*, pp. 1546–1551, 1998.

[12] M. Montemerlo, S. Thrun, D. Koller, and B. Wegbreit, "FastSLAM: A factored solution to the simultaneous localization and mapping problem," in *Proceedings of the Eighteenth AAAI National Conference on Artificial Intelligence*. July 28 - August 1 2002, pp. 1546–1551, AAAI, Edmonton, Alberta, Canada.

[13] J. Nieto, J. Guivant, E. Nebot, and S. Thrun, "Real time data association for fastslam," *Accepted*

*in the IEEE International Conference on Robotics and Automation, ICRA 2003*, September 14-19 2003, Taipei, Taiwan.

[14] J.E. Guivant and E.M. Nebot, "Optimization of the simultaneous localization and map building algorithm for real time implementation," *IEEE Transaction on Robotics and Automation*, vol. 17, no. 3, pp. 242–257, June 2001.

[15] J.E. Guivant and E.M. Nebot, "Improved computational and memory requirements of simultaneous localization and map building algorithms," *IEEE International Conference on Robotics and Automation, ICRA 2002*, p. 27312736, 2002, Washington, USA.

[16] J. Neira and J.D. Tardos, "Data association in stochastic mapping using the joint compatibility test"," *IEEE Transaction of Robotics and Automation*, pp. 890–897, 2001.

[17] J. Gutmann and K. Konolige, "Incremental mapping of large cyclic environments," *IEEE International Symposium on Computational Intelligence in Robotics and Automation CIRA-99, Monterey, CA*, pp. 318–325, November 1999.

[18] S. Thrun, "A probabilistic online mapping algorithm for teams of mobile robots," *International Journal of Robotics Research*, vol. 20, no. 5, pp. 335–363, 2001.

[19] N. J. Gordon, D. J. Salmond, and A. F. M. Smith, "Novel approach to nonlinear/non-gaussian bayesian state estimation," *IEE Proceedings-F*, vol. 140, no. 2, pp. 107–113, Apr. 1993.

[20] M. Isard and A. Blake, "Contour tracking by stochastic propagation of conditional density," *Proc. European Conf. Computer Vision*, pp. 343–356, 1996, Cambridge, Uk.

[21] J. Carpenter, P. Clifford, and P. Fearnhead, "Improved particle filter for nonlinear problems," *IEE Proceedings on Radar, Sonar Navigation*, vol. 146, no. 1, pp. 2–7, February 1999.

[22] S. Lenser and M. Veloso, "Sensor resetting localization for poorly modelled mobile robots," *Proceedings of the IEEE International Conference on Robotics and Automation (ICRA)*, pp. 1225–1232, April 2000, San Francisco, CA.

[23] D. Crisan and A. Doucet, "Convergence of sequential monte carlo methods," Tech. Rep., Technical Report Cambridge University, CUED/FINFENG /TR381, 2000.

[24] J. Guivant, F. Masson, and E. Nebot, "Simultaneous localization and map building using natural features and absolute information," *Journal Robotics and Autonomous Systems*, vol. 40, no. 2-3, pp. 79–90, 2002.

[25] "Experimental outdoor dataset," *http://www.acfr.usyd.edu.au/homepages/academic/enebot/dataset.htm.*